Redox Biology 37 (2020) 101725

Contents lists available at ScienceDirect

Redox Biology

journal homepage: www.elsevier.com/locate/redox

Research Paper

Glutathionylated and Fe–S cluster containing hMIA40 (CHCHD4) regulates ROS and mitochondrial complex III and IV activities of the electron transport chain

Venkata Ramana Thiriveedi [a], Ushodaya Mattam [a,1], Prasad Pattabhi [a,1], Vandana Bisoyi [a], Noble Kumar Talari [a], Thanuja Krishnamoorthy [b], Naresh Babu V. Sepuri [a,*]

[a] Department of Biochemistry, University of Hyderabad, Gachibowli, Hyderabad, TS, 500046, India
[b] Vectrogen Biologicals Pvt.Ltd., BioNEST, School of Life Sciences, University of Hyderabad, Gachibowli, Hyderabad, TS, 500046, India

ARTICLE INFO

Keywords:
MIA40 (CHCHD4)
Electron transport chain
Glutathionylation
Reactive oxygen species
Complex III and IV
Fe–S clusters

ABSTRACT

Human MIA40, an intermembrane space (IMS) import receptor of mitochondria harbors twin CX9C motifs for stability while its CPC motif is known to facilitate the import of IMS bound proteins. Site-directed mutagenesis complemented by MALDI on *in vivo* hMIA40 protein shows that a portion of MIA40 undergoes reversible S-glutathionylation at three cysteines in the twin CX9C motifs and the lone cysteine 4 residue. We find that HEK293T cells expressing hMIA40 mutant defective for glutathionylation are compromised in the activities of complexes III and IV of the Electron Transport Chain (ETC) and enhance Reactive Oxygen Species (ROS) levels. Immunocapture studies show MIA40 interacting with complex III. Interestingly, glutathionylated MIA40 can transfer electrons to cytochrome C directly. However, Fe–S clusters associated with the CPC motif are essential to facilitate the two-electron to one-electron transfer for reducing cytochrome C. These results suggest that hMIA40 undergoes glutathionylation to maintain ROS levels and for optimum function of complexes III and IV of ETC. Our studies shed light on a novel post-translational modification of hMIA40 and its ability to act as a redox switch to regulate the ETC and cellular redox homeostasis.

1. Introduction

The intermembrane space (IMS) of mitochondria is teeming with proteins enriched in disulphide bonds [1]. The disulphide bonds of these proteins enable them to be locked in the IMS. Unlike the proteins bound to the mitochondrial membranes or matrix by dedicated import machinery constituting a plethora of proteins, the IMS proteins are brought in and retained in the IMS by a unique pathway called the disulphide relay pathway [2,3]. The import of the IMS targeted proteins is coupled to their folding and oxidation by the disulphide relay pathway [4,5]. MIA40 (Mitochondrial intermembrane space import and assembly protein 40)/CHCHD4 (coiled-coil-helix-coiled-coil-helix-domain containing 4) and ALR (Augmenter of liver regeneration) are the two important known proteins of this pathway [2,3].

MIA40 is an oxidoreductase that facilitates the import and folding of the IMS targeted proteins by introducing disulphide bonds. ALR (Erv1 in yeast) recycles reduced MIA40 to its oxidized form to initiate another import cycle. The downstream trail of the electrons from ALR reaches the ETC *via* cytochrome C [3,4]. The hydrophobic binding cleft of MIA40 recognizes the substrates to introduce the disulphide bonds and to trigger subsequent folding of the precursor proteins. Additionally, there is a tight coupling between the efficacy of oxidative folding of IMS proteins and their accumulation in the IMS [3,6]. The disulphide relay system prevents the leakage of mature proteins from the IMS [7,8].

MIA40 is a conserved and essential protein. The highly conserved region in human MIA40 (hMIA40) contains six conserved cysteine residues aligned in the order of CPC and two CX9C motifs. The cysteine pair in the CPC motif is implicated in the formation of disulphide bond during the run of the disulphide relay system [9]. At the end of the disulphide relay cycle, ALR, a flavoprotein re-oxidizes the CPC motif of hMIA40 to facilitate a new disulphide relay cycle [10]. The ternary complex formed between a substrate, hMIA40, and ALR is efficient in executing the electron transfer critical for the import, folding, and retention of the substrate i.e., an IMS protein. ALR acts as a redox switch

* Corresponding author. ;
E-mail address: nbvssl@uohyd.ernet.in (N.B.V. Sepuri).
[1] Equally contributed to this work.

https://doi.org/10.1016/j.redox.2020.101725
Received 31 July 2020; Received in revised form 2 September 2020; Accepted 11 September 2020
Available online 15 September 2020

as it accepts an electron pair from MIA40 and transfers two single electrons to two molecules of cytochrome C [10,11].

Maintenance of mitochondrial redox homeostasis is a tightly controlled process as any alterations will affect mitochondrial functioning. Generally, cells use glutathione (GSH) and oxidized glutathione (GSSG) to tweak redox imbalances that frequently occur in the mitochondria that houses the ETC, the main contributor of ROS. GSH is a tripeptide (L-γ-glutamyl-L-cysteinyl-glycine, GSH) that serves as an easily accessible cellular antioxidant that is abundantly present. More recently, it has been re-discovered to S-glutathionylate proteins, a covalent Post Translational Modification (PTM) that competes with other PTMs for its ability to modulate proteins reversibly in diverse cellular pathways like cell growth, cell differentiation, transcription and metabolism during both physiological and mild oxidative stress conditions. Interestingly, GSH accelerates the IMS import process [11]. GSH reduces the formation of long-lived, partially oxidized import intermediates and thereby functions as a proof reader during mitochondrial disulphide relay system [11]. However, it is not clear whether GSH directly interacts with MIA40 or employs glutaredoxin [11].

A recent study shows that AIF, a known mitochondrial apoptotic factor, is required for the biogenesis of respiratory chain complexes. AIF interacts with hMIA40 and regulates respiratory chain biogenesis and the depletion of AIF reduces hMIA40 protein levels in mitochondria by affecting its mitochondrial import. Over-expression of hMIA40 in AIF-depleted cells restores the respiratory chain function, particularly in complex I [12,13]. Also, MIA40 plays a role in the import of specific subunits of respiratory complexes [14]. Thus, the MIA40 mediated pathway can influence the functional state of the respiratory chain complexes [15]. However, the precise mechanism is not known. Besides the known role of MIA40 in the disulphide relay system and the functioning of complexes, we have additionally shown that the CPC motif in MIA40 is capable of binding iron for the export of Fe–S clusters from mitochondria [16].

In the present study, we show that hMIA40 undergoes glutathionylation. Using site-directed mutagenesis and MALDI, we provide evidence that four cysteines within hMIA40 are probable sites for glutathionylation (gt). We generated cysteine mutants (single, double, triple, and quadruple mutants) to understand the physiological significance of gt MIA40 in ROS production and biogenesis of ETC. We find that the cysteine mutants sharply increase cellular ROS production. Besides, the activities of complexes III and IV of the ETC require gt MIA40. These results are further bolstered by our finding that Fe–S clusters present in MIA40 can directly transfer electrons to cytochrome C. Based on the results from this study, we propose a mechanism of action wherein gt MIA40 regulates ROS production by getting glutathionylated to quench ROS and redirecting the electrons to the ETC *via* Fe–S clusters of MIA40 and cytochrome C.

2. Materials and methods

Materials: All chemicals used in this study were purchased from Sigma USA unless otherwise mentioned. Antibodies were purchased from Abcam, USA.

2.1. Plasmid constructions

The h*MIA*40 ORF cDNA was generated using total RNA from HeLa cells as template and primer pairs *MIA40*-Fwd1 (5′-CCCAGAATTCACCATGTCCTATTGCCGGCAGGAA-3′) and *MIA40*-Rev1 (5′-CCACTCGAGTTAACTTGATCCCTCCTCTTCTTT-3′). Total RNA was isolated from HeLa cells using an RNA isolation kit from Bangalore Genei. The h*MIA40* ORF thus generated was used as a template for further amplifying h*MIA40* for cloning into pET28 (a+) vector to generate plasmid pNB130 carrying h*MIA40* wild type with a histidine tag at the N terminus as described earlier [16]. As per manufacturer's protocol, site-directed mutagenesis (Fermentas) was performed on plasmid pNB130 containing wild type h*MIA40* to create plasmids pNB309 (h*MIA40* C53S & C55S), pNB388 (h*MIA40* C4S & C97S), pNB389 (h*MIA40* C4S, C74S & C97S) and pNB390 (h*MIA40* C4S, C64S, C74S & C97S). h*MIA40* wild type and mutants were amplified and cloned into pET28 (a+) and pcDNA3.1 Myc-His vector using *Eco*RI and *Xho*I restriction sites to generate plasmids pNB202 (WT h*MIA40*), pNB314 (h*MIA40* C53S & C55S), pNB379 & pNB388 (h*MIA40* C4S & C97S), pNB380 & pNB389 (h*MIA40* C4S, C74S & C97S), and pNB391 & pNB390 (h*MIA40* C4S, C64S, C74S & C97S) for expression in mammalian and bacterial cells respectively.

2.2. Expression and purification of recombinant proteins

Plasmids pNB130, pNB388, pNB389, and pNB390 were transformed into *E. coli* Rosetta gami SHUFFLE strain. Expression and purification of the recombinant His-hMIA40 wild type and mutant proteins were done as described earlier [16]. Briefly, 1 mM isopropyl-β-D-thiogalactopyranoside (IPTG) was used to induce the expression of recombinant proteins when bacterial cultures attained an OD_{600nm} equal to 0.6. Ni-NTA affinity column (Clontech) used to purify recombinant proteins with Buffer A (50 mM Tris-HCl pH 7.5, 100 mM NaCl, and 1 mM DTT). Buffer A containing 10 mM imidazole was used to wash the column. Buffer A containing 400 mM imidazole used for elution. Experiments associated with Fe–S clusters, purification was carried out at 4 °C using degassed buffers.

2.3. Separation of affinity purified hMIA40 isoforms by gel filtration chromatography and molecular weight cut off filters

Sephadex G100 column used (1.5 × 86 cm, Sigma) for gel filtration of affinity-purified hMIA40. About 100 ml of the gel packed into a glass column, and equilibration carried out with a buffer containing 50 mM Tris-HCl (pH 7.5) and 100 mM NaCl. Calibration of column carried out using standard protein markers such as alcohol dehydrogenase (150 kDa), bovine serum albumin (66 kDa), and carbonic anhydrase (29 kDa). Gel filtration of hMIA40 was carried out at room temperature using the equilibration buffer. 2 ml fractions collected as eluates and their absorbance recorded at 280 nm by using a UV–Vis spectrophotometer (Hitachi-2910).

The oligomeric (~70 kDa and above), dimeric (~35 kDa), and monomeric (22 kDa) forms of hMIA40 initially identified by gel filtration, were also separated with a molecular weight cut off filter tubes (Amicon centrifugal filters, Millipore). Affinity-purified recombinant hMIA40 subjected to centrifugal filtration. A 50 kDa filter initially used to enrich the higher oligomeric forms, while the flow-through contained the dimeric and monomeric forms. The flow-through subjected further to 30 kDa cut off filter to separate the dimeric form (retained in the tube) and the monomeric form (flow-through). All the forms of MIA40 suspended in a degassed buffer containing 50 mM Tris-HCl (pH 7.5), 100 mM NaCl and 1 mM DTT. The enriched fractions containing different forms of MIA40 were directly used for presence of Fe–S clusters or dialyzed in the absence of DTT and stored at −20 °C with 20% glycerol.

2.4. UV absorption spectroscopy analysis

Recombinant proteins and their various forms were monitored for their UV–Vis absorption (300 nm–700 nm) in a Hitachi U-2910 spectrophotometer with the help of a quartz cuvette of 1 cm path length at room temperature. For monitoring Fe–S clusters, proteins analyzed for presence of characteristic Fe–S cluster absorption peak either at 410 and, or 460 nm.

2.5. Cell culture and transfection for binding to GSH sepharose

HEK293T cells were cultured in complete Dulbecco's modified Eagle's medium (Invitrogen) containing 10% (v/v) fetal calf serum at 37 °C

under an atmosphere of 5% CO_2. Cells were grown in 100 mm and 175 mm flasks transfected with 8 μg and 20 μg respectively of scrambled shRNA or human *MIA40* shRNA plasmid (ORIGENE) by using lipofectamine transfection reagent (Invitrogen). HEK293T cells co-transfected with mammalian expression pcDNA3.1 plasmids harboring Myc-His-h*MIA40* wild type or mutants (pNB202; pNB314; pNB380; and pNB391) along with *MIA40* shRNA to partially inhibit endogenous h*MIA40* expression. Cells, thus transfected, were used for GSH binding and other studies.

2.6. Isolation of mitochondria from HEK293T cells

Isolation of mitochondria from rat liver mitochondria [17,18] and HEK293T cell lines were done as described earlier [19]. Briefly, HEK293T cells were washed once with phosphate-buffered saline (PBS) and harvested in mitochondria isolation buffer (20 mM HEPES pH 7.5, 1.5 mM $MgCl_2$, 1 mM EDTA pH 8.0, 1 mM EGTA, 210 mM sucrose, and 70 mM mannitol). The cell suspension was homogenized using polytron 1600 (5 sec X 2 pulses and 15 rpm). The partially homogenized cell suspension was subjected further to Dounce homogenization. The homogenate was centrifuged at 1000×*g* for 10 min at 4 °C. The supernatant was centrifuged again at 10,000×*g* for 15 min at 4 °C. The pellet fraction containing mitochondria was washed twice and suspended in a buffer containing 250 mM sucrose, 5 mM magnesium acetate, 40 mM potassium acetate, 10 mM sodium succinate, 1 mM DTT, and 20 mM HEPES-KOH, pH 7.4.

2.7. Immunoprecipitation

For carrying out the immunoprecipitation studies using HEK293T cells, transfection was done with mammalian expression vector pcDNA3.1 c-Myc-His or vector containing h*MIA40* ORF. Cells were grown for 6 h in serum-free DMEM medium before adding a complete medium. 24 h post-transfection, cells were treated with 10 mM NAC for 12 h. Cells were washed with PBS and lysed in NP-40 buffer (50 mM Tris-HCl pH 8.0, 150 mM NaCl, 1% Nonidet P-40, and 1X protease inhibitor cocktail). Immunoprecipitation carried out overnight using an antibody against GSH, followed by the addition of protein A sepharose beads and incubation for 4 h at 4 °C on a rotator. Washing of beads done with NP-40 buffer and elution with 2X Laemmli's sample buffer. Eluates subjected to reducing SDS PAGE, Western transferred, and blots probed with the hMIA40 antibody.

2.8. Complex III & IV immunoprecipitation

Mouse monoclonal antibody against complex III (ab109862, Abcam) and complex IV (ab109801, Abcam) used to immuno-precipitate complex III and IV [20]. Briefly, 500 μg of mitochondria isolated from the HEK293T cells expressing hMIA40 and QM mutant solubilized in a buffer A (PBS with 20 mM dodecyl maltoside) and incubated on ice for 30 min followed by centrifugation at 70,000×*g* for 30 min.

To the supernatant, 10 μg of complex III or IV immuno-capture antibody was added. The samples incubated at 4 °C overnight on a rotator. Next, protein A sepharose beads added, and further incubation carried out for 4 h at 4 °C on a rotator. Later, beads were washed twice with 1 mL of buffer A and complex III or IV associated proteins eluted with 2 × Laemmli's sample buffer. Eluates were subjected to NuPAGE 4–12% Bis-Tris gel (Invitrogen) using MES as a running buffer (50 mM 2-morpholinoethanesulfonic acid, 50 mM Tris base, 0.1% SDS, 1 mM EDTA) at 100 V for 2–3 h. The gels were western transferred and probed with hMIA40, cytochrome C, and complex III immuno-capture antibody.

2.9. GSH pull down assay

Transfected HEK293T cells were allowed to grow for 6 h in serum-free DMEM medium before the addition of complete medium. 24 h post-transfection, cells were treated with increasing concentration of H_2O_2 (25, 50, and 100 μM) for 30 min [21,22]. Next, cells were lysed with modified NP-40 buffer (150 mM NaCl, 1% NP-40, 50 mM Tris-HCl pH 8.0, and 2 mM EDTA), centrifuged at 10,000 rpm and the supernatants collected. Similarly, mitochondria isolated from rat liver or un-transfected HEK293T cells lysed in NP40 buffer. The lysates were incubated on a rotator along with glutathione sepharose beads and 1X protease inhibitor cocktail (Roche) for 1 h at room temperature (RT). Beads were washed thrice with NP-40 buffer before elution with 2X Laemmli's sample buffer. Samples were resolved on SDS PAGE, Western blotted, and blots probed with specified antibodies.

2.10. In vitro GSH pull down assay

In case of pre-treatment before GSH pull down, samples containing 50 μg of recombinant and purified His-hMIA40 protein were pre-treated at RT with various concentrations of DTT (1, 5, 10, and 20 mM) for 30 min or with H_2O_2 (1, 2, and 5 mM) for 1 h. In the case of pre-treatment with both DTT and H_2O_2, pre-treatment was carried out sequentially. 20 mM iodoacetamide (IAA) was added at the end of pre-treatment to block any free thiols. Next, 30 μl of GSH-Sepharose beads were added to all the samples, and the mixtures incubated further on a rotator for 1 h at RT. In the absence of pre-treatment, 200 μg of recombinant and purified His-hMIA40 wild type or mutants were directly incubated with beads in Tris buffer containing 1X protease inhibitor cocktail. Beads were washed thrice with Tris buffer (50 mM Tris-HCl pH7.5, 100 mM NaCl) (pre-treatment samples) or Tris buffer with 1 mM GSH followed by elution with Tris buffer containing 10 mM DTT (pre-treatment samples) or 20 mM GSH. The eluates were subjected to SDS-PAGE, Western transferred, and the blots probed with the hMIA40 antibody.

2.11. Mitochondrial complex activities

(a) Mitochondrial complex I activity analyzed by measuring NADH oxidation to NAD^+ at 340 nm [23]. Briefly, 30 μg of 0.05% Triton X 100 treated mitochondria incubated with 100 μM NADH in a buffer containing 50 mM potassium phosphate pH 7.5, 5 mM $MgCl_2$, and 0.25% BSA for 2 min. The activity of complex I was initiated by the addition of 60 μM decylubiquinone, and the decrease in absorption at 340 nm was measured. Using the velocity of reaction (Δabsorption/min) and the molar extinction coefficient of NADH (3.4 $mM^{-1}cm^{-1}$ at 340 nm with reference wavelength), the activity of complex I calculated.

(b) Mitochondrial complex II activity was monitored spectrophotometrically at 600 nm [23]. Briefly, mitochondria (30 μg) was solubilized in 0.05% Triton X 100 and incubated in 25 mM potassium phosphate buffer containing 20 mM succinate at 37 °C for 10 min. Complex II activity initiated by the addition of 80 μM 2, 6-dichlorophenolindophenol (DCPIP), and the decrease in absorption at 600 nm was measured. The blue color of oxidized DCPIP turns colorless when it accepts an electron from complex II. Complex II activity calculated using the velocity of reaction and the molar extinction coefficient of DCPIP ($19.1 mM^{-1}cm^{-1}$).

(c) Mitochondrial complex III activity analyzed by measuring the cytochrome C reduction at 550 nm [23]. Briefly, 30 μg of 0.05% Triton X 100 treated mitochondria incubated in 25 mM potassium phosphate buffer pH 7.4 containing 2 mM NaN_3 and 50 μM cytochrome C. Addition of 50 μM reduced decylubiquinone (DBH_2), initiates complex III activity and the increase in absorption at 550 nm for 2 min measured. Cytochrome C is brown in its oxidized state, and that turns orange-pink when it accepts an electron from complex III. Complex III activity calculated using the velocity of reaction (Δabsorbance/min) and the molar extinction coefficient of cytochrome C (18.5 $mM^{-1}cm^{-1}$ at 550 nm with reference wavelength). Beer-Lambert law equation used to calculate the complex III activity.

(d) Mitochondrial complex IV activity analyzed by measuring cytochrome C oxidation at 550 nm [23]. Briefly, 50 μM of reduced cytochrome C incubated in 50 mM potassium phosphate buffer pH 7.4. Complex IV activity initiated by the addition of 30 μg of 0.05% Triton X 100 treated mitochondria and the decrease in absorbance at 550 nm for 2 min was measured. Cytochrome C reduction performed by adding tiny amounts of sodium dithionite until the absorbance of reduced cytochrome C at 550 nm is between 1.8 and 1.9. Complex IV activity calculated using the velocity of reaction (Δabsorbance/min) and the molar extinction coefficient of cytochrome C (18.5 $mM^{-1}cm^{-1}$ at 550 nm with reference wavelength). Complex IV activity calculated using the Beer-Lambert law equation.

2.12. Reduction of cytochrome C by hMIA40

Gel filtered and fraction separated oligomer, dimer and monomer forms of recombinant purified hMIA40, unfractionated MIA40, CPC mutant, and QM mutant proteins were incubated (80 μg, 3.6 μM final concentration) with 10 μM oxidized cytochrome C in 50 mM potassium phosphate buffer pH 7.4. Reduction of cytochrome C can be followed by monitoring the absorbance at 550 nm for 10 or 30 min in a Hitachi U-2910 spectrophotometer at RT or monitoring the UV–Visible spectra (200–700 nm) using a quartz cuvette of 1 cm path length. The brown color of oxidized cytochrome C changes to orange-pink upon reduction.

2.13. ROS measurement

ROS was measured using the fluorescent dye H_2DCF-DA. Post transfection, HEK293T cells were incubated with 25 μM DCF-DA for 45 min at 37 °C. Next, cells were washed with PBS and harvested. The emission fluorescence measured using fluorescence spectroscopy with maximum excitation and emission spectra of 495 nm and 529 nm, respectively.

2.14. MALDI-TOF LC-MS/MS

MALDI-TOF LC-MS/MS performed to detect cysteine modifications of hMIA40. Gt peptide peaks can be distinguished in MALDI-TOF spectra by the corresponding 306 Da (approximate GSH molecular weight) increase in molecular weight at cysteine residues. Trypsin-digested peptides were separated by BECH18 (2.1mmx150mmx1.7 μm dimension) column and run on the SynaptG2 QTOF instrument for MS/MS analysis and the data received from the instrument analyzed by PLGS (protein lynx global server) software.

2.15. Circular Dichroism spectroscopy

For recombinant hMIA40 and QM mutant of hMIA40, Circular Dichroism performed in a Jasco J-815 spectrophotometer with quartz cuvettes of 0.1 cm path length. Spectra was documented at 20 °C from 200 to 260 nm wavelength with a determination of 1.0 nm and an acquisition time of 50 nm/min. The final spectra obtained by averaging three repeated scans [24].

2.16. Statistical analysis

All statistical analyses performed using Jandel Scientific Sigma stat software by one way ANOVA followed by Post hoc Dunkan's test for multiple comparisons and alterations between two groups with Students t-test.

3. Results

3.1. Glutathionylation of hMIA40

Mitochondria is dependent on the import of nuclear-encoded proteins for its biogenesis and maintenance, and the disulphide relay system is vital and integral to the mitochondrial protein import. A recent observation shows that this pathway is not limited to the import of IMS proteins but extends to membrane proteins. GSH reduces the partially oxidized import intermediates that have outlived their time and thereby ensure fidelity to the process. However, there is no clarity on the mechanism of its action and the apparently coordinated interplay between GSH and MIA40. Given the proximity of GSH and MIA40, the common substrates, presence of multiple cysteines in MIA40, and their functional overlap, we hypothesized that MIA40 could be a potential substrate for S-glutathionylation.

Binding of proteins to GSH sepharose beads would indicate the presence of reactive cysteines in the protein, an indicator for potential glutathionylation [25–27]. Cell extracts from HEK293T cells were passed through GSH-sepharose beads, as indicated in the methods and the eluates probed with antibodies against the proteins mentioned (Supplementary Figure: S1). We find that proteins that are prone to glutathionylation (GAPDH, tubulin, aconitase, actin, and ABCB7) efficiently bound to the column while HSP70 fails to bind to the column indicating the specificity of the assay. Hence, we assessed for reactive cysteine presence in recombinant purified MIA40 as well as in MIA40 from HEK293T cells.

Recombinant purified MIA40 was pre-treated with either increasing concentrations of DTT (1–20 mM) to reduce the reactive cysteines (Fig. 1A) or H_2O_2 (1–5 mM) (Fig. 1B) before binding to GSH sepharose beads as described in the methods section. Beads were washed, eluted, and loaded on SDS-PAGE, Western blotted and probed with an antibody against MIA40. Recombinant MIA40 is observed to harbor reactive cysteines as it binds to GSH sepharose beads; however, this binding decreases with increasing concentration of DTT pre-treatment while H_2O_2 has the opposite effect. We repeated this experiment using lysates from HEK293T cells transiently transfected with Myc-His-h*MIA40* construct or vector control. Cells were pre-treated with H_2O_2 (25–100 μM), as described in the methods. An equivalent amount of lysates were used (Fig. 1D) for binding studies with GSH-sepharose beads (Fig. 1C). Reduced and oxidized forms of hMIA40 are observed (Fig. 1D) [28]. The binding of native MIA40 is faint; however, with over-expression, we detect binding that is further improved with H_2O_2 pre-treatment. This result is consistent with the assessment using recombinant MIA40 that MIA40 has a mixture of reactive and latent cysteines and that H_2O_2 can activate the latter. We had resorted to over-expressing MIA40 in HEK293T cells to determine the glutathionylation as its endogenous levels are low. However, to establish that endogenous MIA40 is indeed glutathionylated, we repeated the experiment using extracts of isolated rat liver mitochondria (Fig. 1E) and lysates from HEK293T cells (Fig. S1). We find that a fraction of endogenous MIA40 efficiently binds to GSH-sepharose, while ALR used as a control fails to bind to it (Fig. 1E). These results show that the native, endogenous MIA40 protein is prone to glutathionylation, albeit at a low level.

N-acetyl-L-cysteine (NAC) can act as a precursor for GSH synthesis intracellularly. If indeed MIA40 is getting gt under normal physiological conditions, we should expect an increase in its glutathionylation with an increase in GSH levels. To confirm the glutathionylation of MIA40, we initially grew HEK293T cells in the presence of an increasing concentration of NAC for 12 h. We used HEK293T cells transiently transfected with Myc-His-h*MIA40* construct or vector alone. Transfected cells were used instead of native cells to improve the sensitivity of the immunoprecipitation assay with GSH antibody and the blots probed with MIA40 antibody. We find MIA40 pulled down with the GSH antibody and its binding affinity increasing with an increase in NAC treatment (Fig. 1F). The transfected cell lysates were monitored for the steady-state

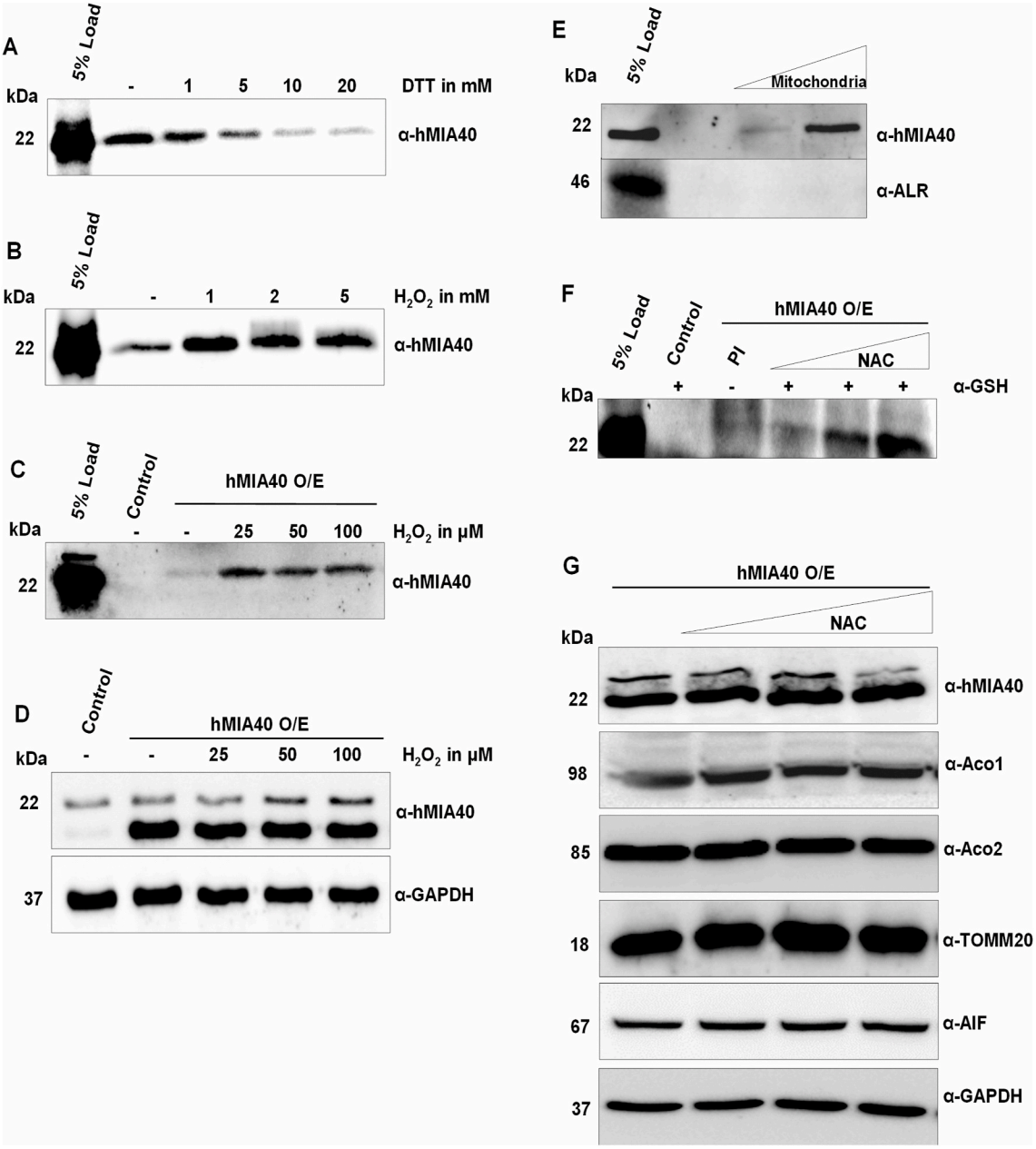

Fig. 1. hMIA40 harbors reactive cysteines. (A) Recombinant and purified hMIA40 protein was treated with increasing concentration of DTT (1, 5, 10, and 20 mM) for 30 min before pull down with GSH-sepharose beads as described under Methods. After elution, GSH sepharose beads were resolved on SDS-PAGE and western blotted. Immunoblot probed with the hMIA40 antibody is shown. (B) It is the same as in (A) except that instead of DTT, increasing concentrations of H_2O_2 (1, 2, and 5 mM) used. (C) Lysate of HEK293T cells over-expressing hMIA40 were treated with increasing concentration of H_2O_2 (25, 50, and 100 μM) before pull-down with GSH-sepharose beads and processed as described in (A). Control indicates HEK293T cells transfected with vector. (D) Lysates (50 μg) from (C) before GSH pull-down were loaded on to SDS-PAGE and Western blotted. The immunoblot was probed with MIA40 and GAPDH antibodies to show the expression level of MIA40. (E) increasing concentrations (1 and 2 mg) of mitochondrial extracts from rat liver used for GSH pull-down assay and probed with MIA40 and ALR (F) Lysate of HEK293T cells over-expressing hMIA40 were treated with increasing concentration of NAC (1, 5 and 10 mM) for 12 h before immunoprecipitation with GSH antibody or pre-immune serum (PI) or no antibody (control) and binding to protein A sepharose beads. After resolution on SDS-PAGE and western blotting, the immunoblot probed with the hMIA40 antibody. (G) Lysates (50 μg) from (F) before immunoprecipitation resolved on SDS-PAGE, Western blotted, and the blots probed with antibodies against hMIA40, Aco1, Aco2, TOMM20, AIF, and GAPDH.

expression level of hMIA40, mitochondrial and cytosolic proteins after exposure to NAC. The protein levels are comparable in cells expressing Myc-hMIA40 in the presence and absence of NAC (Fig. 1G). Taken together, the results above clearly show that a fraction of MIA40 undergoes glutathionylation.

3.2. Glutathionylation on hMIA40 is reversible

Having ascertained that hMIA40 has reactive cysteines, we examined if recombinant and purified hMIA40 are enriched in GSH and whether it can undergo glutathionylation *in vitro*. Unlike the reduced form of hMIA40 that exists as a monomer, its oxidized form can attain multiple forms ranging from a pure monomer to a dimer to an oligomer. If indeed hMIA40 is enriched with GSH, it would be interesting to discern the

relationship between glutathionylation and the structural form of hMIA40. We initially resolved purified recombinant hMIA40 on a non-reducing and a reducing SDS-PAGE; and stained the gels with Coomassie (Fig. 2A). In the absence of a reducing agent, hMIA40 is found to be in two primary monomeric forms, a fast migrating oxidized form and a slower migrating reduced form (Fig. 2A, lane 1). Also, we find other high molecular weight forms that likely represent the dimeric, trimeric, and oligomeric forms of oxidized MIA40 (Fig. 2A, lane 1) as described [16,28,29]. In the presence of a reducing agent, all the high molecular weight bands disappear, and the majority of MIA40 migrates as a reduced monomer (Fig. 2A, lane 2). To test if recombinant hMIA40 protein is enriched in GSH, increasing concentrations of recombinant MIA40 protein (0.5, 1, & 1.5 μg) were separated on a non-reducing SDS-PAGE, Western transferred, and the blots probed with antibodies against GSH and MIA40 (Fig. 2B & C). GSH antibody detects two prominent bands of molecular weights 33 and 52 kDa along with some high molecular weight bands. These protein bands likely represent the dimeric, trimeric, and higher molecular weight oligomeric forms of MIA40 (Fig. 2B and C). Recombinant purified hMIA40 is found to be gt inherently and shows that it can exist in multiple structural forms. Pre-treatment with increasing concentrations of H_2O_2 moderately increases the oligomerization without compromising on the glutathionylation status (Fig. 2D).

In contrast, pre-treatment with increasing DTT concentrations and β-mercaptoethanol completely reduces hMIA40 to its monomeric form (Fig. 2F). Importantly, β-mercaptoethanol removes the GSH moiety from hMIA40 (Fig. 2F and G). These results demonstrate that recombinant hMIA40 is post-translationally modified by glutathionylation, and oxidizing agents preserve glutathionylation in hMIA40 by promoting their oligomerization. Potent reducing agents like β-mercaptoethanol not only completely monomerize hMIA40 but also deglutathionylates hMIA40.

3.3. Four cysteines in MIA40 are prone to glutathionylation

hMIA40 harbors seven cysteines clustered in the CPC (C53, C55) and two CX9C (C64, C74, C87, C97) motifs besides present as C4. MALDI-TOF LC-MS/MS (hereafter, MALDI) analysis used to ascertain the

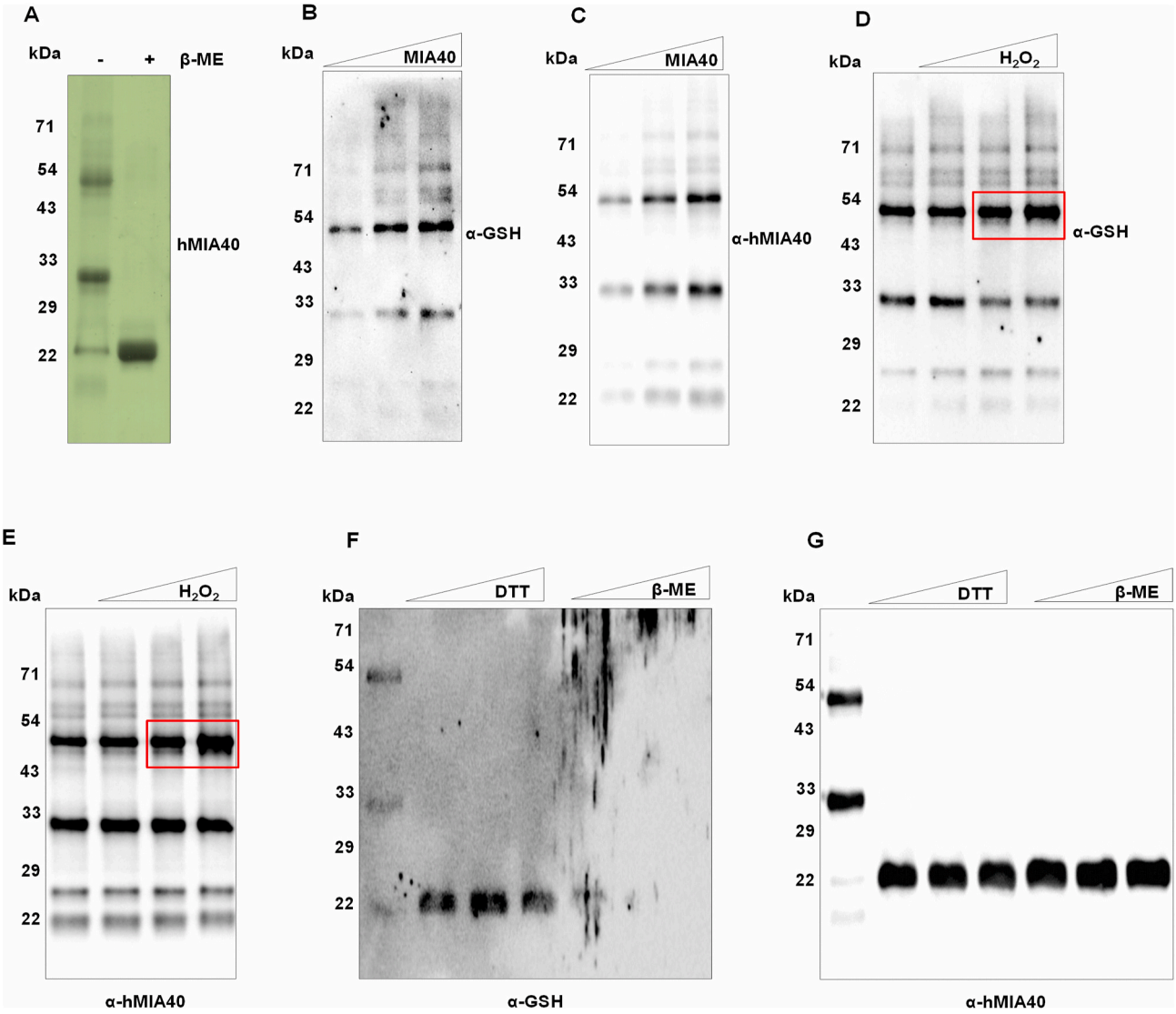

Fig. 2. Glutathionylation of MIA40 is reversible. (A) Recombinant purified hMIA40 (10 μg) was resolved on a non-reducing and reducing SDS-PAGE and Coomassie-stained. (B&C) Increasing concentrations of recombinant hMIA40 (0.5, 1, & 1.5 μg) were resolved on a non-reducing SDS-PAGE, western transferred, and the blots probed with GSH and hMIA40 antibodies. (D&E) Same as in B&C, however, hMIA40 (10 μg) was treated with increasing concentrations of H_2O_2 (1, 2, and 5 mM) for 60 min before their resolution on a non-reducing SDS-PAGE. (F&G) Same as in D&E, however, hMIA40 (2 μg) was pre-treated with increasing concentrations of DTT (1, 5, and 10 mM) or β-mercaptoethanol (100, 150, and 200 mM) instead of H_2O_2.

reactive cysteines and glutathionylation in hMIA40. HEK293T cells over-expressing Myc-His-hMIA40 were harvested for carrying out GSH pull-down assay as described in the Methods. The proteins bound to GSH-sepharose were resolved on a non-reducing SDS-PAGE along with recombinant His-hMIA40 and the gel Coomassie-stained (Supplementary Fig. S2). The ~22 kDa band corresponding to over-expressed Myc-His-hMIA40 (using recombinant hMIA40 as reference), was excised, trypsin digested, and subjected to MALDI analysis (Fig. 3). C4, C64, C74, and C97 appear to be gt while the cysteines in CPC motif and C87 in the CX9C motif appear to be insensitive to glutathionylation.

To further establish that C4, C64, C74, and C97 are indeed gt, we resorted to site-directed mutagenesis studies to generate double (C4S, C97S, henceforth *MIA40* DM), triple (C4S, C74S, C97S, henceforth *MIA40* TM), and quadruple (C4S, C64S, C74S, C97S, henceforth *MIA40* QM) *MIA40* mutants (Fig. 4A). *E. coli* cells transformed with the plasmids, and the over-expressed recombinant His-MIA40 wild type and mutants were affinity purified using Ni-NTA beads as described in the Methods. An equal amount of recombinant MIA40 proteins used for carrying out affinity pull-down using GSH-sepharose beads as described above. Western blots were probed with the MIA40 antibody. Recombinant wild type His-MIA40 having all the reactive cysteines can efficiently bind GSH beads. However, the binding capacity of MIA40 decreases with an increase in substitutions at the reactive cysteines. Despite the presence of intact cysteines in the CPC motif and of C87, binding of His-MIA40 QM to GSH sepharose is almost abolished (Fig. 4B). There is a possibility that hidden cysteines in recombinant MIA40 get exposed in Rosetta cells due to improper folding and permit binding to GSH beads. To rule out this possibility, we also expressed and purified the recombinant wild type and QM MIA40 from the SHUFFLE strain. Disulfide bond isomerase (DsbC) in the SHUFFLE strain promotes proper folding of proteins. An equivalent amount of wild type and QM MIA40 proteins were passed through the GSH-sepharose beads, and the eluates analyzed. We find that while wild type MIA40 binds efficiently to GSH beads, QM MIA40 binds sparingly (Supplementary Fig. S3). Besides, we carried out CD studies on purified recombinant proteins MIA40 wild type and QM expressed in Rosetta gami cells to check their folding status as described in the Methods. We find minor changes in the secondary structure of the mutant (Supplementary Figs. S4A and S4B).

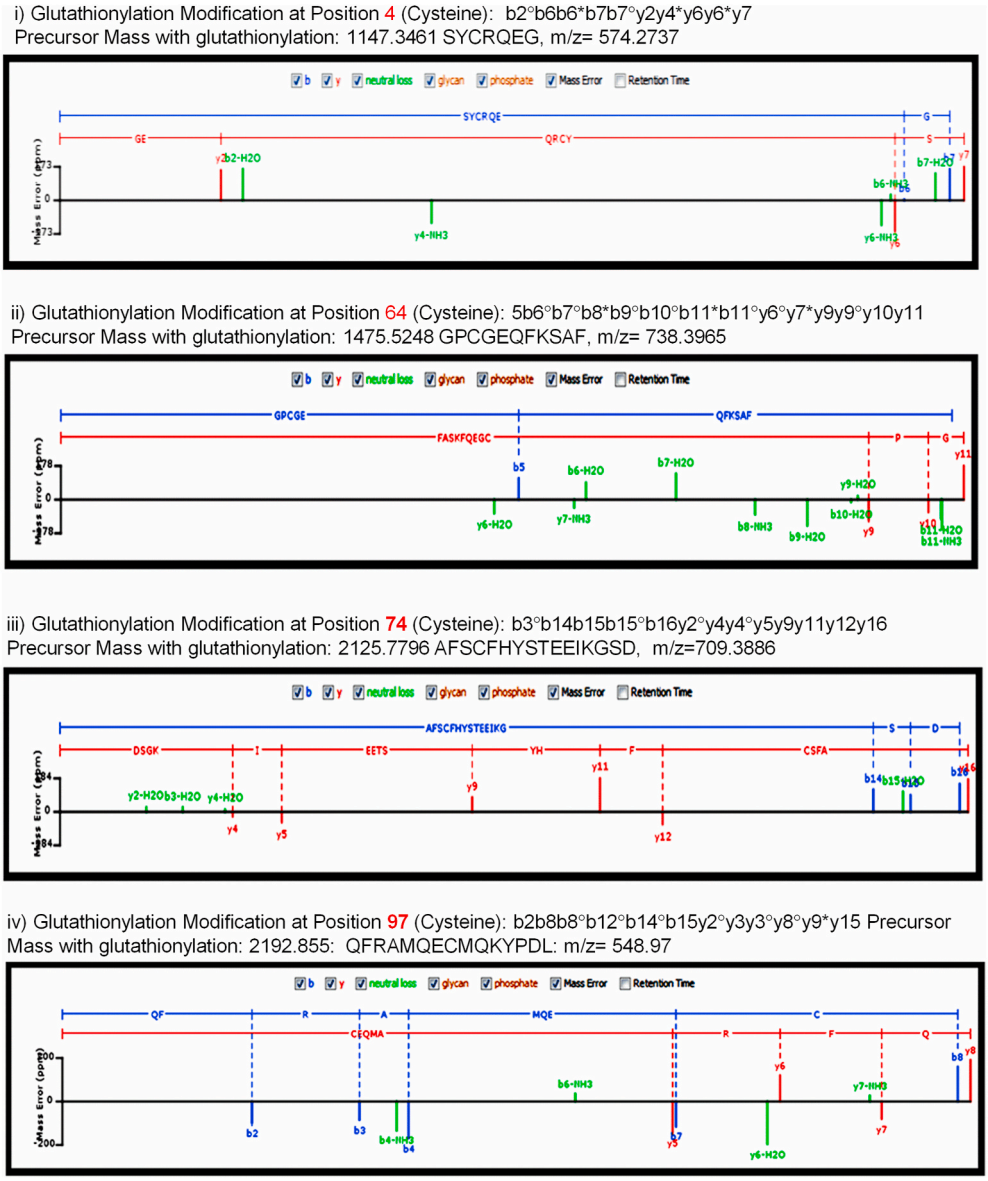

Fig. 3. Four cysteines in MIA40 are Glutathionylated. Lysate of HEK293T cells over-expressing Myc-His-hMIA40 was treated with 10 mM NAC before pull-down with GSH sepharose beads. After washing and elution, beads subjected to a non-reducing SDS-PAGE, and the gel Coomassie-stained. A 22 kDa band corresponding to hMIA40 kDa excised and subjected to MALDI analysis. LC-MS/MS analysis of gt cysteine peaks spectrum.

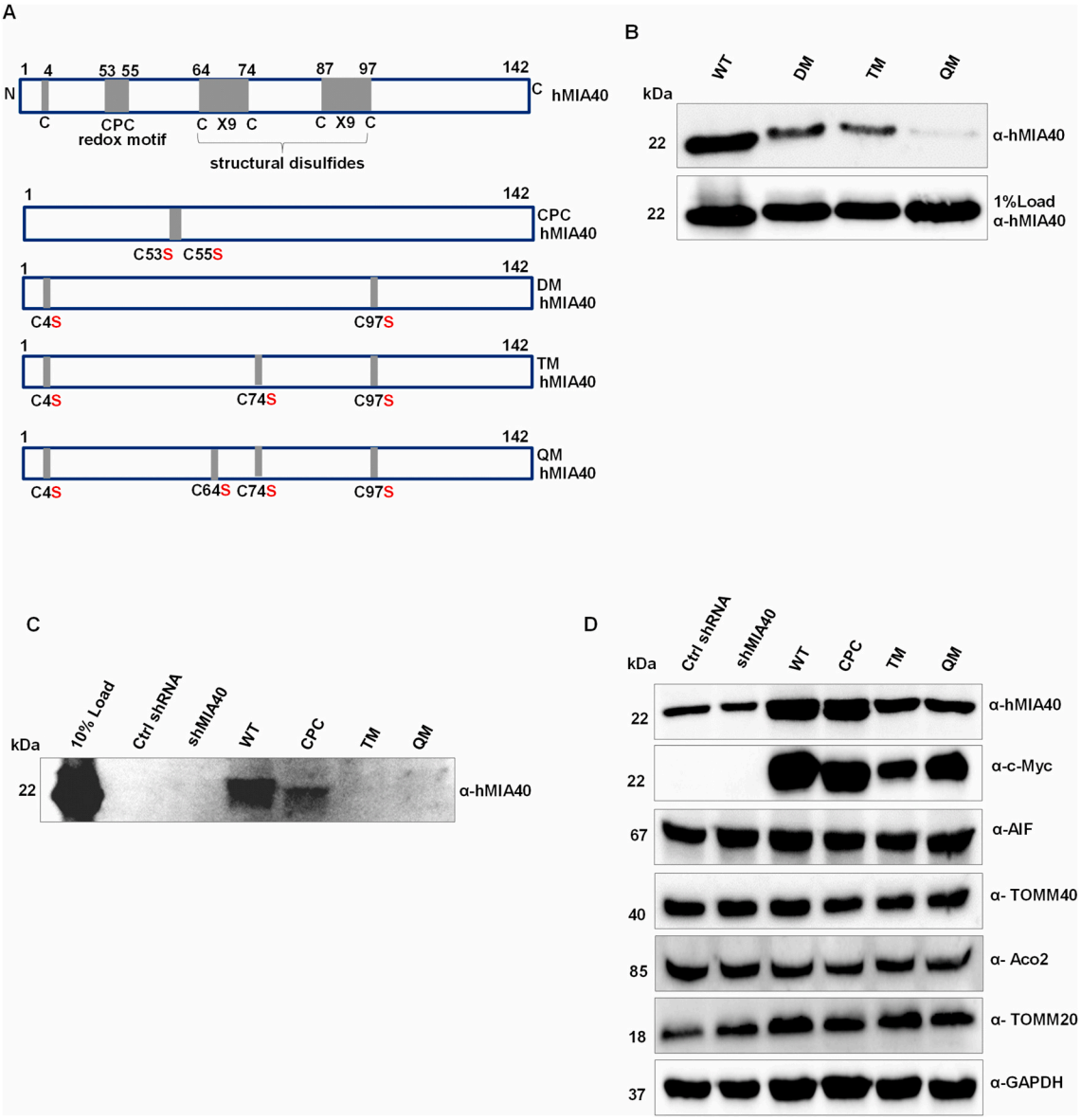

Fig. 4. Validation of gt cysteines in hMIA40. (A) Schematic representation of the hMIA40 amino acid sequence shows the CPC and the dual CX9C motifs besides the seven cysteine positions. It additionally depicts the various cysteine to serine mutations generated by site-directed mutagenesis. (B) Recombinant hMIA40 wild type, DM, TM, and QM were purified from bacteria and used in GSH-sepharose pull-down as described in the Methods. Following SDS-PAGE and western blotting of the samples, the blots probed with the hMIA40 antibody. (C) HEK293T cells were co-transfected with scrambled shRNA and plasmid over-expressing Myc-His-hMIA40 wild type, CPC mutant, TM, or QM. Post-transfections, cells were treated with 10 mM NAC for 12 h before pull-down with GSH-sepharose beads. Samples resolved on SDS-PAGE, Western blotted, and the blots probed with hMIA40 antibody. (D) Lysates (50 μg) of transfected HEK293T cells from (C) were subjected to SDS-PAGE and western blotting before GSH-sepharose pull-down. The blots probed with antibodies against hMIA40, Myc, Aco2, TOMM20, TOMM40, AIF, and GAPDH.

These results demonstrate that hMIA40 is gt *in vivo* at four cysteine sites, and it is imperative that C4, C64, C74, and C97 be present for maximum glutathionylation.

We replicated the *in vitro* GSH-sepharose binding studies using the whole repertoire of cysteine to serine hMIA40 mutants expressed in HEK293T cells. Endogenous expression of h*MIA40* in HEK293T was silenced partially by transfecting cells with shRNA specific against endogenous h*MIA40*, while cells were concomitantly co-transfected with pcDNA3.1 plasmids hosting Myc-His-h*MIA40* wild type or h*MIA40* TM and h*MIA40* QM mutants. After 24 h post-transfection, an equal number of cells were treated with 10 mM NAC for 12 h, followed by cell lysis as described in the Methods section. Lysates resolved on SDS-PAGE, Western blotted, and probed with hMIA40 antibody to measure the shRNA mediated reduction in endogenous hMIA40. Around 30–40% reduction in endogenous expression of h*MIA40* achieved compared to control cells transfected with random shRNA (Fig. 4D). A three to four-fold over-expression of wild type and CPC (C53S–C55S) mutant of Myc-His-*MIA40* was observed compared to the endogenous control level (Fig. 4D). However, cells transfected with Myc-His-*MIA40*TM and QM construct had relatively lower expression (Fig. 4D). A plausible reason for the dip in the over-expression of the triple and quadruple mutants is increased degradation triggered by structural instability [29]. GSH-sepharose pull-down assay was carried out using the above lysates, and the results essentially re-confirmed the MALDI and *in vitro* results (Fig. 4C). hMIA40 wild type has the innate ability to bind to GSH-Sepharose due to its reactive cysteines (Fig. 1A,B,1C, 4B, and 4C). Cysteine residues at positions 4, 64, 74, and 97 are instrumental in conferring this capability to MIA40 while the cysteines in the CPC motif are not involved (Fig. 4C). We also monitored the steady-state protein levels of several mitochondrial proteins in the lysates to

ensure that there are no non-specific effects (Fig. 4D). The GSH assays using hMIA40 mutants provide convincing evidence that indeed hMIA40 is gt *in vivo*, and four of the seven cysteines within it are gt *in vivo*.

3.4. Gt hMIA40 regulates ETC biogenesis and ROS production

For the first time, we show that a fraction of hMIA40 is getting gt *in vivo*. To gain insights into the physiological consequences of this post-translational modification, we looked at its chaperone role in the assembly of inner mitochondrial membrane protein complexes of the vital ETC. We speculated that the cysteines' glutathionylation in MIA40 might improve its effect on the ETC complex assembly and function. To check if this is true, we monitored the steady-state levels of the various ETC complex proteins in HEK293T cells over-expressing Myc-His-MIA40 wild type and mutants (CPC motif mutant; TM and QM). Mitochondrial samples from the shRNA and pcDNA3.1 co-transfected cells were resolved on SDS-PAGE, Western blotted, and probed with the OXPHOS antibody. OXPHOS antibody is a combination of antibodies that can detect five significant components of complexes I, II, III, IV, and V of ETC. Components of complex 1 (NDUFB8), II (SDHB), and IV (MTCO1) have reduced steady-state levels in the mitochondria isolated from cells expressing h*MIA40* TM and QM besides control cells wherein h*MIA40* is partially silenced compared to cells expressing wild type h*MIA40*, or its CPC mutant version (Fig. 5A and B).

This outcome depicts a direct correlation between the depletion of hMIA40 or glutathionylation of hMIA40 and the protein level of the components of ETC complexes, in particular, complex I, II, and IV. As a follow up to this finding, we were curious to look at the efficiency and activity of the individual complexes that constitute the ETC in the above mitochondrial samples. Surprisingly, in the case of complexes I and II activities, all the samples had comparable activity despite the over-expression of wild type and mutant h*MIA40* or partial silencing of endogenous h*MIA40* (Fig. 5C and D). However, complex III activity is sensitive to partial silencing of endogenous h*MIA40* as the activity decreases by half in cells transfected with only h*MIA40* shRNA (Fig. 5E). Correspondingly, complex III activity is augmented in cells over-expressing h*MIA40* wild type or the CPC mutant. However, cells over-expressing h*MIA40* TM or QM have compromised complex III activity compared to cells over-expressing wild type h*MIA40* (Fig. 5E). The pattern of complex IV activity mimics that of complex III except that there is a dramatic reduction of this activity in cells over-expressing all the mutants of h*MIA40*, including the CPC mutant, and the effect is much more pronounced in the QM mutant (Fig. 5F). These results provide evidence that hMIA40 modulates complex III and complex IV activities to influence the ETC.

Most importantly, cysteines in MIA40 that are prone to glutathionylation are crucial for both complex III and complex IV activities while the latter is additionally sensitive to the overall structure of hMIA40. The activities of complexes I and II are not affected despite a decline in their steady-state levels, as mentioned above. A possible explanation could be that the cells still had the required levels for optimum activity despite the observed reduction in their protein levels.

As the ETC is the production site for ROS and hMIA40 regulates ETC complexes, we measured ROS in the cells over-expressing h*MIA40* wild type and its mutants. Partial silencing of endogenous h*MIA40* leads to a three-fold increase in ROS (Fig. 5G). In corollary, over-expression of h*MIA40* wild type decreases ROS's level to a lower level than in control cells. Over-expression of h*MIA40* CPC, TM, and in particular, QM increases the ROS levels. Our results reveal, for the first time, a hitherto unappreciated link between hMIA40 and ROS production that impacts redox homeostasis.

Intriguingly, either over-expression or depletion of MIA40 affects the complex III activity without altering their protein levels significantly. It suggests that MIA40 might be regulating complex III activity. To address this hypothesis, we carried out immuno-capture studies of complexes III and IV in lysates over-expressing wild type and QM MIA40, as described in the Methods section. Both MIA40 wild type and QM mutant interact with complex III (Fig. 5H and I) but not complex IV (Fig. S5). These studies indicate that MIA40 may be a conduit for channeling electrons from complex III to cytochrome C.

3.5. hMIA40 transfers electrons to cytochrome C

In the ETC assembly line, cytochrome C accepts electrons from complex III and mitochondrial intermembrane relay systems to deliver complex IV. As the activities of both complex III and IV decreased in the *MIA40* mutants, we reasoned that cytochrome C's function must be compromised. To validate this reasoning, we assessed cytochrome C activity using purified recombinant hMIA40 wild type and mutant proteins *in vitro*. hMIA40 requires ALR/Erv1 to act as an intermediate for transferring electrons to cytochrome C using an indirect oxygen consumption assay [30]. We developed a simple assay wherein one can directly monitor the reduction of oxidized cytochrome C in a spectrophotometer. Oxidized cytochrome C was incubated with reduced and dialyzed hMIA40 proteins, and the reduction of oxidized cytochrome C was followed by monitoring the UV–visible spectra from 200 to 700 nm.

Cytochrome C reduction can be monitored by the appearance of the prominent α and β peaks, and the subtle movement of the gamma peak to the right. The addition of sodium dithionite, a known reducing agent, efficiently reduces cytochrome C (Fig. 6A). Curiously, we find that reduced recombinant wild type hMIA40 is capable of reducing cytochrome C efficiently without the requirement of ALR (Fig. 6B). However, all the mutants of hMIA40 that were tested (QM and CPC) have significantly reduced activity, with the CPC mutant being completely defective in reducing oxidized cytochrome C (Fig. 6B). Additionally, we also followed the reduction of oxidized cytochrome C temporally for 30 min at 550 nm. Consistent with the earlier observations, we find that wild-type hMIA40 reduces cytochrome C in a time-dependent manner while the CPC and QM mutants fail to reduce cytochrome C (Fig. 6C).

During protein import, MIA40 transitions from a reduced to oxidized to reduced form by donating the pair of electrons taken from the imported protein to the ALR protein. The ALR protein, however, uses its FAD domain to donate one electron at a time to the heme-Fe present in the cytochrome C. The reduction of cytochrome C directly by MIA40 seeks a molecular explanation on the trajectory of the electron pathway. We and others have shown earlier that the CPC domain of MIA40 holds Fe–S clusters [16,31]. We hypothesized that MIA40 might employ its Fe–S clusters to transfer an electron to cytochrome C in a fashion similar to the FAD domain of ALR. In addition, MIA40 can exist in multiple forms depending on its oxidation status. To test our hypothesis, we first separated the various forms of MIA40 by two methods to ascertain the structural form enriched in Fe–S clusters. Purified recombinant MIA40 was subjected to Sephadex-100 gel filtration chromatography and also to Amicon cut-off filtration, as described in the Methods. Gel filtration separates MIA40 as an oligomer (P1), dimer (P2), and monomer (P3) (Fig. S6). Similarly, we rapidly obtained three different fractions by utilizing a 30 kDa and 50 kDa cut off filters.

Interestingly, unlike gel filtration oligomer fraction, Amicon purified oligomer fraction contains all the forms (oligomer, dimer, and monomer) of MIA40 on a native gel. However, all the fractions either separated by gel filtration or Amicon method migrate as a single monomer under reduced conditions (Supplementary Figs. S7 and S8). The presence of Fe–S clusters was monitored spectrophotometrically (absorption at 410 or 460 nm) in the presence of a reducing agent as described earlier [16]. Fe–S clusters are detected in the oligomer and dimer fractions obtained by the Amicon method (Fig. 6D); however, none of the gel filtration fractions have Fe–S clusters indicating the transient and labile nature of Fe–S clusters on MIA40. The purified fractions obtained through Amicon filtration were dialyzed to remove the reducing agent and further tested for their ability to reduce cytochrome C. Curiously; we find that only the oligomeric fraction can reduce cytochrome C more

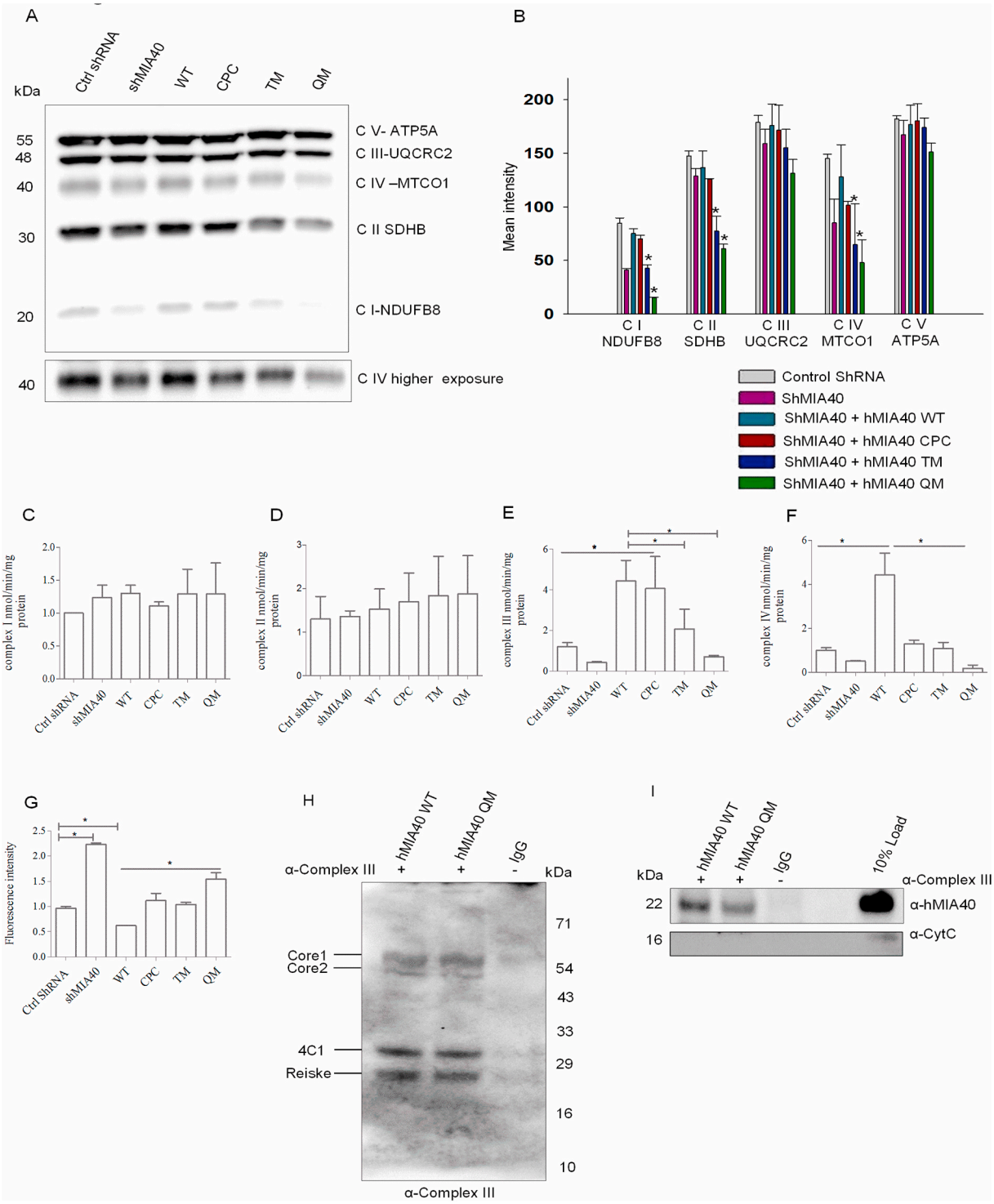

Fig. 5. Gt-hMIA40 regulates the ETC biogenesis and ROS production. Lysates of HEK293T transfected cells used as above. (A) Mitochondria were isolated, resolved on SDS-PAGE and western blotted. The blots probed with OXPHOS antibody that can detect significant components of ETC such as complex I (NDUFB8, 20 kDa), complex II (SDHB, 30 kDa), complex III (UQCRC2, 48 kDa), complex IV (MTCO1, 40 kDa) and complex V (ATP5A, 55 kDa) as shown (B) Quantification of blots from three independent experiments, (C, D, E & F) Activities of complexes I, II, III, and IV of ETC were analyzed spectrophotometrically as described in the Methods section and shown here. (G) ROS levels were measured in HEK293T transfected cells by H_2DCFDA method, as described in the methods. All results plotted with mean ± S. E. (n = 3), $*P \leq 0.05$. (H) Mitochondria of HEK293T cells over-expressing hMIA40 WT and QM mutant were used for immunocapture of complex III or pre-immune serum (PI) or no antibody (control) and binding to protein A sepharose beads. After resolution on SDS-PAGE and western blotting, the immunoblot probed with the Complex III antibody (H) and hMia40 and Cytochrome C (I).

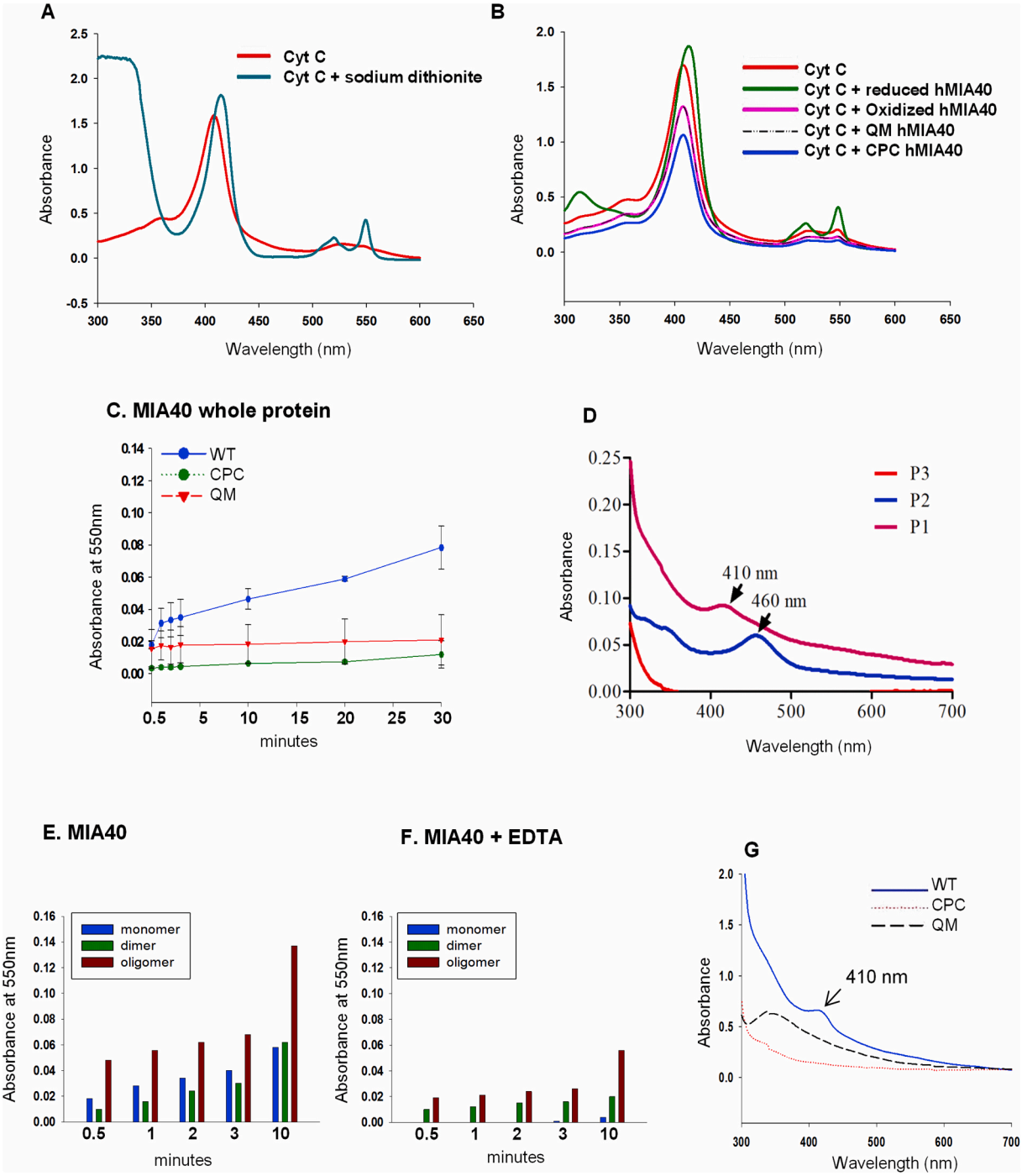

Fig. 6. hMIA40 reduces cytochrome C. (A) Oxidized cytochrome C (10 μM) was incubated with sodium dithionite in a buffer (50 mM potassium phosphate buffer pH7.4 and 0.5 mM EDTA) for 5 min before being scanned for absorption in the UV–visible spectral region. Shown here is a scan. (B) Recombinant hMIA40 wild type and mutant versions were over-expressed and affinity-purified from bacteria using Ni-NTA beads. 80 μg of the purified proteins were incubated with 10 μM oxidized cytochrome C as described in the Methods. The ability of hMIA40 wild type and mutant proteins to reduce oxidized cytochrome C was monitored in a Hitachi spectrophotometer by following the UV–visible spectra. (C) Oxidized cytochrome C incubated with 80 μg of wild type hMia40, CPC motif mutant hMIA40, and QM mutant hMIA40 in a buffer (50 mM potassium-phosphate buffer pH7.4) and cytochrome C reduction measured at 550 nm. (D) UV–Vis spectra of P1 (oligomer), P2 (dimer), and P3 (monomer) samples obtained after fractionation of his-hMia40. (E) Oxidized cytochrome C incubated with 80 μg of the oligomer, dimer, and monomer in a buffer (50 mM potassium-phosphate buffer pH7.4) and cytochrome C reduction measured at 550 nm. (F) Oxidized cytochrome C incubated with 80 μg of the oligomer, dimer and monomer in a buffer (50 mM potassium-phosphate buffer pH7.4 and 0.5 mM EDTA) and cytochrome C reduction measured at 550 nm. (G) UV–Vis spectra of wild type hMIA40, CPC mutant hMIA40, and QM mutant hMIA40 showing Fe–S absorption peak.

efficiently in a time-dependent manner compared to dimer and monomer fractions (Fig. 6E). Examination of the dialyzed MIA40 fractions for Fe–S clusters revealed that only the oligomeric fraction retained Fe–S clusters, albeit to a lesser extent than before dialysis; however, the dimer had lost most of the Fe–S clusters (Fig. S9). This explains the inability of the dialyzed dimer fraction to reduce cytochrome C. To directly investigate the role of Fe–S clusters in the reduction of cytochrome C, we repeated the cytochrome reducing assay in the presence of EDTA, a

metal chelating agent. EDTA abolishes the reduction of cytochrome C by oligomeric MIA40 (Fig. 6F).

In contrast, in agreement with our results, both M4 and CPC mutants are bereft of Fe–S clusters and likewise cannot reduce cytochrome C (Fig. 6C and G). The above results show that Fe–S clusters play a critical role in reducing cytochrome C by hMIA40.

4. Discussion

MIA40, a synonym for CHCHD4 (Coiled-coil-helix-coiled-coil-helix domain-containing protein 4), is imported from the cytoplasm into the mitochondrial IMS. It is assigned the function of folding small cysteine-containing mitochondrial IMS bound proteins for their import and retention. We have shown earlier that it has an essential role as a component of the mitochondrial Fe–S cluster export machinery. In this study, we show that hMIA40 can undergo post-translational modification by getting gt at four cysteines C4, C64, C74, and C97. Intriguingly, the CPC motif is bereft of any glutathionylation, while three cysteine residues in the twin CX9C motifs are gt. Interestingly, we and others have shown that the CPC motif of MIA40 binds to Fe [16,31]. We demonstrate that glutathionylation and Fe–S clusters of hMIA40 have critical physiological consequences that affect cellular respiration and redox homeostasis. hMIA40 defective in glutathionylation or Fe–S clusters, increases ROS, decreases the activities of complexes III and IV of the ETC, and is unable to reduce oxidized cytochrome C.

The cysteines in CX9C motifs form stable disulphide bridges and provide structural stability to MIA40. The redox status of mitochondria might likely influence the cysteines' glutathionylation in a fraction of MIA40 (Fig: 1, 2, and S1). Since endogenous steady-state levels of MIA40 are low, we over-expressed MIA40 protein in HEK293T cells for our studies. It is possible that a fraction of over-expressed MIA40 in the cytosol is in an un-oxidized state and exposes hidden structural cysteines to bind to GSH-sepharose beads. However, majority of over-expressed cytoplasmic hMIA40 is always in an oxidized and folded state, and the glutaredoxins or AIF facilitate their entry into the mitochondrial IMS [11,32–34]. Consistent with this, a published study from our lab has shown that most of the over-expressed MIA40 protein is efficiently targeted to mitochondria in HEK293T cells [16].

Further, specific pull-down of a small amount of recombinant wild type MIA40 indicates the presence of two distinct populations of MIA40. We cannot completely rule out the possibility that unfolded MIA40 undergoes glutathionylation. However, the specific pull-down of wild type MIA40 and not QM MIA40 protein expressed in the SHUFFLE strain using GSH-sepharose column and the results from CD spectral studies rule out a significant improper distortion reason in the mutant protein but rather implicate the lack of cysteines (Figure: S3 & S4).

4.1. Regulation of ETC by MIA40

A previous study has shown that depletion of MIA40 reduces the subunits of complexes I to IV of the ETC to various degrees [35]. However, in our studies, there is a moderate reduction in the oxphos subunits of complexes I, II and IV in shRNA, TM and QM mutant cells as the cells still retain 70% of the MIA40 endogenous pool. The endogenous MIA40 may be sufficient for the import of IMS and specific subunits of membrane proteins. Nevertheless, the decrease in membrane proteins may be attributed to an additional layer of regulation required for their integration and stabilization that is compromised in MIA40 mutant cells.

The protein subunits of ETC complexes maintain specific stoichiometric ratios that are critical for their function. The selective decrease in complexes III and IV activities is intriguing. It is possible that as MIA40 has a role in the protein import of the subunits of ETC complex proteins, the absence of gt might influence the composition and stoichiometry of the complexes. On the other hand, changes in the ETC complexes may be compensated by PTMs such as phosphorylation to enable their integration and assembly. MIA40 might be facilitating the proper flow of electrons by quenching the ROS from complex III and delivering to complex IV *via* cytochrome C. Immunocapturing experiments results show that indeed MIA40 interacts with complex III (Fig. 5H and I), but not complex IV (Fig. S5). Complexes I and III are the primary sites for ROS production, and as complex I activity is not affected in our studies, we believe that the increase in ROS generation is due to perturbed complex III function in our mutants.

4.2. 2 Electron to 1 electron transfer

ALR can transfer electrons to cytochrome C due to the presence of a prosthetic Flavin moiety. Our *in vitro* results suggest that MIA40 is capable of donating electrons directly to cytochrome C. How can MIA40, a two-electron carrier, transfer electrons to cytochrome C, a single electron acceptor? Our studies implicate the Fe–S clusters present in the CPC motif of MIA40 oligomers in the transfer of electrons to cytochrome C (Fig. 6C). Glutathionylation leads to oligomerization, and Fe–S clusters are relatively more stably associated with oligomers. Nevertheless, the CPC motif is critical for the electron transfer function of Fe–S clusters as CPC mutant is defective in reducing cytochrome C though glutathionylated. We have successfully separated the oligomeric, dimeric, and monomeric forms of MIA40 by fractionation. The rather labile and transient association of the Fe–S clusters with the non-oligomeric forms of MIA40 might explain their relatively lower cytochrome C reduction activity. Importantly, we show that the Fe–S clusters in MIA40 facilitate the two-electron to one-electron transfer to reduce cytochrome C (Fig. 6C and E).

Also, MIA40 does not interact with Complex IV directly but affects its activity because of its upstream action on Complex III and cytochrome C. This outcome indicates a possible functional linkage of CPC mutant to complex IV activity (Fig: 5E). We believe that hMIA40 tends to dimerize and oligomerize to facilitate the transfer of electrons from the glutathionylated cysteines to Fe–S clusters containing CPC motifs (Fig. 7). Interestingly, the QM mutant deficient in Fe–S clusters (Fig. 6G) and latent cysteines acts like a dominant negative mutant and display weak complex III and IV activities besides failing to reduce cytochrome C. This result links cysteines, glutathionylation, oligomerization and Fe–S clusters of MIA40 to ETC function (Fig. 7).

4.3. Glutathionylation and ROS

Redundancy of pathways provides flexibility and failsafe mechanism to sustain critical processes in the face of potential damage. ETC is crucial for energy production, and cells must be employing multiple electron acceptors and intermediates. Interestingly, Erv1/ALR transfers electrons directly to oxygen to form H_2O_2 [36]. However, during anaerobic conditions, fumarate reductase (Osm1) transfers the electrons from Erv1 to fumarate in the IMS [37]. Based on our investigations, we firmly believe that the function of hMIA40 is not limited to the import of proteins into IMS or the export of the Fe–S cluster but undergoes post-translational modification to sustain the ETC (Fig. 5).

Mitochondria acts as a hub for ROS production, which is a physiological by-product for many of the metabolic activities. Increased ROS production is associated with several pathological conditions such as cancer, diabetes mellitus, atherosclerosis, ischemia and other mitochondria-related abnormalities [38–44]. The cell efficiently uses it as a signaling molecule when it is at a low level; however, it succumbs to it when its level increases. Mitochondria continually adapt to the dynamic redox environment due to flux changes in ROS by modulating the function of its proteins through oxidation of protein cysteine thiols. The importance of glutathionylation as a PTM has recently gained more traction. It is considered a '*bona fide*' redox signal as it can modulate protein function *in vivo* by modifying it reversibly, swiftly, and in a highly specific manner, fulfilling all the criteria for an efficient and vital PTM [45]. Several proteins from varying biological pathways, including metabolic and mitochondrial protein import, have been identified to

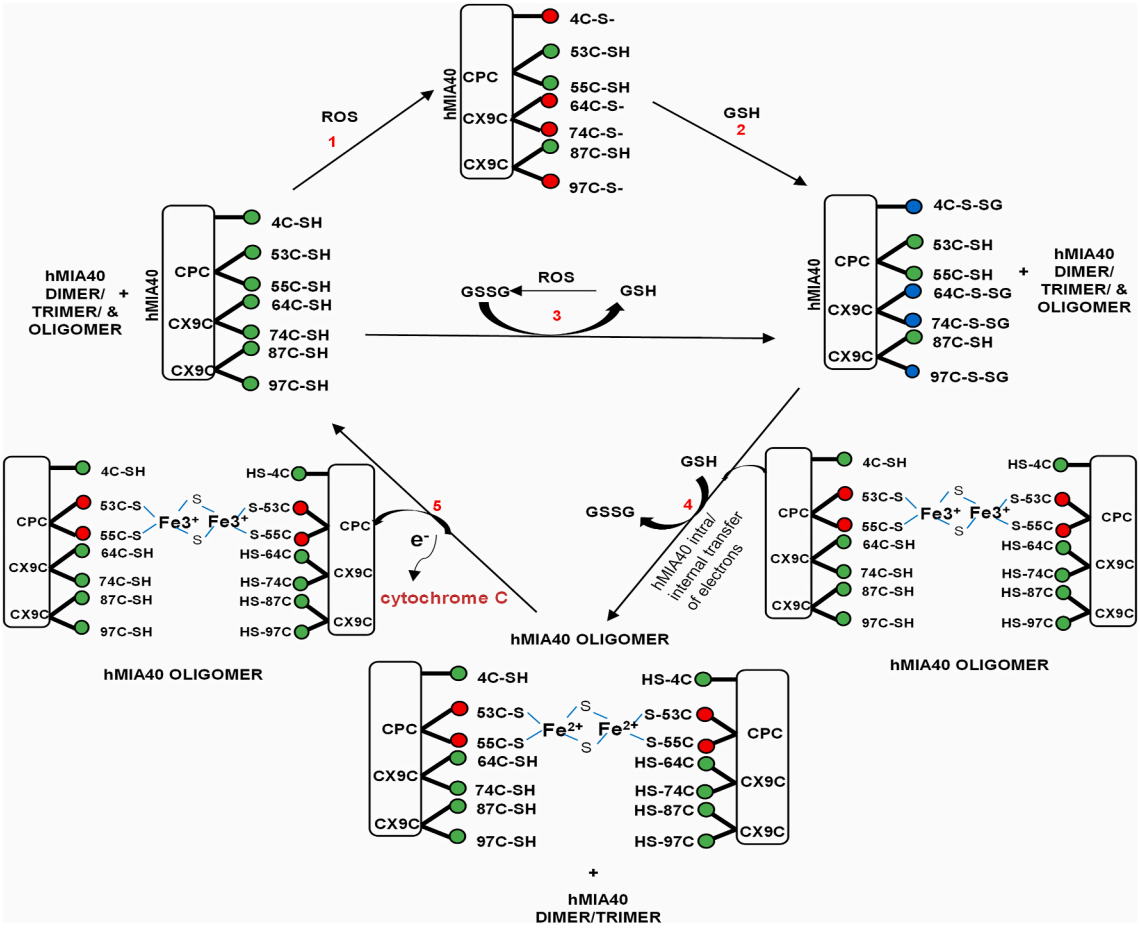

Fig. 7. A proposed mechanistic scheme depicting the glutathionylation of MIA40 and transfer of electrons to cytochrome C. 1 & 2. ROS activates the reactive cysteines that subsequently get glutathionylated by GSH 3. ROS oxidizes GSH to GSSG. GSSG glutathionylates MIA40. 4. MIA40 gets deglutathionylated by the transfer of electrons to Fe–S motif present in CPC intramolecularly. 5. It accesses another CPC motif by dimerization/oligomerization in order to transfer another pair of electrons. The high molecular weight MIA40 gets reduced by transferring electrons to cytochrome C *via* Fe bound to CPC motif and monomerizes, and CPC motif forms disulfides. CPC motif reduces probably through protein import.

undergo glutathionylation. Reactions involving glutathionylation are susceptible to oxidized and reduced GSH levels driven by the cellular ROS. Glutathionylation of proteins is now considered a hallmark for stress response, and any defects in this can lead to pathological conditions. MIA40 could act as a repository for ROS by getting gt and transferring back the electrons to the ETC to mitigate ROS's toxic effects. 30% reduction in MIA40 increases ROS by several folds (Fig. 5G). Because of the biological outcomes of protein glutathionylation associated with stress, they serve as potential biomarkers for stress-related human diseases. The concept of cells having a 'redoxome' wherein protein cysteine thiols act as sensors for the surrounding redox environment is being appreciated. Jones and Sies have recently suggested the existence of a 'redox code' determined by the redox flux generated by the cellular metabolic activities, bioenergetics, and the health of the anti-oxidant systems [46]. Given that proteins can undergo a multitude of redox modifications, glutathionylation being just one, and the paucity of information on the molecular mechanism behind these modifications, further studies will unravel the redox world.

Declaration of competing interest

The authors declare that they have no conflicts of interest with the contents of this article.

Acknowledgement

We acknowledge Science and Engineering Research Board (SERB) of India [grant number CRG/2018/001028] for funding to N.B.V.S.Laboratory, a Department of Science and Technology Fund for Improvement of S&T Infrastructure grant to the Department of Biochemistry, a UGC-DRS grant to Department of Biochemistry and DBT-Builder grant to School of Life Sciences. ICMR, India for SRF fellowship to VR. Thiriveedi. We thank Monica Kannan and Sandor Lifesciences, Hyderabad for carrying out proteomic studies and all the members of N.B.V.S. Laboratory for their comments and suggestions.

Appendix A. Supplementary data

Supplementary data to this article can be found online at https://doi.org/10.1016/j.redox.2020.101725.

References

[1] M. Deponte, K. Hell, Disulphide bond formation in the intermembrane space of mitochondria, J. Biochem. 146 (2009) 599–608, https://doi.org/10.1093/jb/mvp133.

[2] K. Hell, The Erv1-Mia40 disulfide relay system in the intermembrane space of mitochondria, Biochim. Biophys. Acta 1783 (2008) 601–609. https://doi.org/10.1016/j.bbamcr.2007.12.005.

[3] N. Mesecke, N. Terziyska, C. Kozany, F. Baumann, W. Neupert, K. Hell, J. M. Herrmann, A disulfide relay system in the intermembrane space of

mitochondria that mediates protein import, Cell 121 (2005) 1059–1069, https://doi.org/10.1016/j.cell.2005.04.011.
[4] Y. Finger, J. Riemer, Protein import by the mitochondrial disulfide relay in higher eukaryotes, Biol. Chem. 401 (2020) 749–763, https://doi.org/10.1515/hsz-2020-0108.
[5] M. Habich, J. Riemer, Stop wasting protein—proteasome inhibition to target diseases linked to mitochondrial import, EMBO Mol. Med. 11 (2019) e10441, https://doi.org/10.15252/emmm.201910441.
[6] J.M. Müller, D. Milenkovic, B. Guiard, N. Pfanner, A. Chacinska, Precursor oxidation by Mia40 and Erv1 promotes vectorial transport of proteins into the mitochondrial intermembrane space, Mol. Biol. Cell 19 (2008) 226–236, https://doi.org/10.1091/mbc.E07-08-0814.
[7] A. Chacinska, C.M. Koehler, D. Milenkovic, T. Lithgow, N. Pfanner, Importing mitochondrial proteins: machineries and mechanisms, Cell 138 (2009) 628–644, https://doi.org/10.1016/j.cell.2009.08.005.
[8] D.P. Sideris, K. Tokatlidis, Trapping oxidative folding intermediates during translocation to the intermembrane space of mitochondria: in vivo and in vitro studies, Methods Mol. Biol. 619 (2010) 411–423, https://doi.org/10.1007/978-1-60327-412-8_25. Clifton, N.J.
[9] D. Stojanovski, P. Bragoszewski, A. Chacinska, The MIA pathway: a tight bond between protein transport and oxidative folding in mitochondria, Biochim. Biophys. Acta Mol. Cell Res. 1823 (2012) 1142–1150, https://doi.org/10.1016/j.bbamcr.2012.04.014.
[10] V.N. Daithankar, S.R. Farrell, C. Thorpe, Augmenter of liver regeneration: substrate specificity of a flavin-dependent oxidoreductase from the mitochondrial intermembrane space, Biochemistry 48 (2009) 4828–4837, https://doi.org/10.1021/bi900347v.
[11] M. Bien, S. Longen, N. Wagener, I. Chwalla, J.M. Herrmann, J. Riemer, Mitochondrial disulfide bond formation is driven by intersubunit electron transfer in Erv1 and proofread by glutathione, Mol. Cell 37 (2010) 516–528, https://doi.org/10.1016/j.molcel.2010.01.017.
[12] E. Hangen, O. Féraud, S. Lachkar, H. Mou, N. Doti, G.M. Fimia, N. vy Lam, C. Zhu, I. Godin, K. Muller, A. Chatzi, E. Nuebel, F. Ciccosanti, S. Flamant, P. Bénit, J. L. Perfettini, A. Sauvat, A. Bennaceur-Griscelli, K. Ser-Le Roux, P. Gonin, K. Tokatlidis, P. Rustin, M. Piacentini, M. Ruvo, K. Blomgren, G. Kroemer, N. Modjtahedi, Interaction between AIF and CHCHD4 regulates respiratory chain biogenesis, Mol. Cell 58 (2015) 1001–1014, https://doi.org/10.1016/j.molcel.2015.04.020.
[13] C. Reinhardt, G. Arena, K. Nedara, R. Edwards, C. Brenner, K. Tokatlidis, N. Modjtahedi, AIF meets the CHCHD4/Mia40-dependent mitochondrial import pathway, Biochim. Biophys. Acta (BBA) - Mol. Basis Dis. 1866 (2020) 165746, https://doi.org/10.1016/j.bbadis.2020.165746.
[14] A.J. Erdogan, J. Riemer, Mitochondrial disulfide relay and its substrates : mechanisms in health and disease, Cell Tissue Res. 367 (2017) 59–72, https://doi.org/10.1007/S00441-016-2481-z.
[15] S. Allen, V. Balabanidou, D.P. Sideris, T. Lisowsky, K. Tokatlidis, Erv1 mediates the Mia40-dependent protein import pathway and provides a functional link to the respiratory chain by shuttling electrons to cytochrome c, J. Mol. Biol. 353 (2005) 937–944, https://doi.org/10.1016/j.jmb.2005.08.049.
[16] A. Murari, V.R. Thiriveedi, F. Mohammad, V. Vengaldas, M. Gorla, P. Tammineni, T. Krishnamoorthy, N.B.V. Sepuri, Human mitochondrial MIA40 (CHCHD4) is a component of the Fe-S cluster export machinery, Biochem. J. 471 (2015) 231–241, https://doi.org/10.1042/BJ20150012.
[17] P. Tammineni, C. Anugula, F. Mohammed, M. Anjaneyulu, A.C. Larner, N.B. V. Sepuri, The import of the transcription factor STAT3 into mitochondria depends on GRIM-19, a component of the electron transport chain, J. Biol. Chem. 288 (2013) 4723–4732, https://doi.org/10.1074/jbc.M112.378984.
[18] N.B.V. Sepuri, M. Gorla, M.P. King, Mitochondrial Lysyl-tRNA synthetase independent import of tRNA lysine into yeast mitochondria, PLoS One 7 (2012) 1–8, https://doi.org/10.1371/journal.pone.0035321.
[19] F. Mohammed, M. Gorla, V. Bisoyi, P. Tammineni, N.B.V. Sepuri, Rotenone-induced reactive oxygen species signal the recruitment of STAT3 to mitochondria, FEBS (Fed. Eur. Biochem. Soc.) Lett. 594 (2020) 1403–1412, https://doi.org/10.1002/1873-3468.13741.
[20] B. Schilling, J. Murray, C.B. Yoo, R.H. Row, M.P. Cusack, R.A. Capaldi, B. W. Gibson, Proteomic analysis of succinate dehydrogenase and ubiquinol-cytochrome c reductase (Complex II and III) isolated by immunoprecipitation from bovine and mouse heart mitochondria, Biochim. Biophys. Acta (BBA) - Mol. Basis Dis. 1762 (2006) 213–222, https://doi.org/10.1016/j.bbadis.2005.07.003.
[21] J.W. Zmijewski, S. Banerjee, H. Bae, A. Friggeri, E.R. Lazarowski, E. Abraham, Exposure to hydrogen peroxide induces oxidation and activation of AMP-activated protein kinase, J. Biol. Chem. 285 (2010) 33154–33164, https://doi.org/10.1074/jbc.M110.143685.
[22] Y. Lee, J. Choi, K.H. Ha, D.M. Jue, Transient exposure to hydrogen peroxide inhibits the ubiquitination of phosphorylated IκBα in TNFα-stimulated HEK293 cells, Exp. Mol. Med. 44 (2012) 513–520, https://doi.org/10.3858/emm.2012.44.8.058.
[23] M. Spinazzi, A. Casarin, V. Pertegato, L. Salviati, C. Angelini, Assessment of mitochondrial respiratory chain enzymatic activities on tissues and cultured cells, Nat. Protoc. 7 (2012) 1235–1246, https://doi.org/10.1038/nprot.2012.058.
[24] A. Marada, S. Karri, S. Singh, P.K. Allu, Y. Boggula, T. Krishnamoorthy, L. Guruprasad, N.B. V Sepuri, A single point mutation in mitochondrial Hsp70 cochaperone Mge 1 gains thermal stability and resistance, Biochemistry 55 (2016) 7065–7072, https://doi.org/10.1021/acs.biochem.6b00232.
[25] T. Adachi, R.M. Weisbrod, D.R. Pimentel, J. Ying, V.S. Sharov, C. Schoneich, R. A. Ccohen, S-glutathiolation by peroxynitrite activates SERCA during arterial relaxation by nitric oxide, Nature Medicine 10 (2004) 1200–1207, https://doi.org/10.1038/nm1119.
[26] S.K. Niture, C.S. Velu, N.I. Bailey, K.S. Srivenugopal, S.- Thiolation mimicry, Quantitative and kinetic analysis of redox status of protein cysteines by glutathione-affinity chromatography, Arch. Biochem. Biophys. 444 (2005) 174–184, https://doi.org/10.1016/j.abb.2005.10.013.
[27] C.S. Velu, S.K. Niture, C.E. Doneanu, N. Pattabiraman, K.S. Srivenugopal, R. V. March, V. Re, M. Recei, V. April, Human p53 is inhibited by glutathionylation of cysteines present in the proximal DNA-binding domain during oxidative stress, Biochemistry 46 (2007) 7765–7780, https://doi.org/10.1021/bi700425y.
[28] A.J. Erdogan, M. Ali, M. Habich, S.L. Salscheider, L. Schu, C. Petrungaro, L. W. Thomas, M. Ashcroft, L.I. Leichert, L. Prates, J. Riemer, Redox Biology the mitochondrial oxidoreductase CHCHD4 is present in a semi-oxidized state in vivo, Redox Biol. 17 (2018) 200–206, https://doi.org/10.1016/j.redox.2018.03.014.
[29] S. Hofmann, U. Rothbauer, N. Mühlenbein, K. Baiker, K. Hell, M.F. Bauer, Functional and mutational characterization of human MIA40 acting during import into the mitochondrial intermembrane space, J. Mol. Biol. 353 (2005) 517–528, https://doi.org/10.1016/j.jmb.2005.08.064.
[30] S.K. Ang, H. Lu, Deciphering structural and functional roles of individual disulfide bonds of the mitochondrial sulfhydryl oxidase Erv1p, J. Biol. Chem. 284 (2009) 28754–28761, https://doi.org/10.1074/jbc.M109.021113.
[31] M.P. Spiller, S.K. Ang, E. Ceh-Pavia, K. Fisher, Q. Wang, S.E.J. Rigby, H. Lu, Identification and characterization of mitochondrial Mia40 as an iron-sulfur protein, Biochem. J. 455 (2013) 27–35, https://doi.org/10.1042/BJ20130442.
[32] L. Banci, I. Bertini, C. Cefaro, S. Ciofi-Baffoni, A. Gallo, M. Martinelli, D.P. Sideris, N. Katrakili, K. Tokatlidis, MIA40 is an oxidoreductase that catalyzes oxidative protein folding in mitochondria, Nat. Struct. Mol. Biol. 16 (2009) 198–206, https://doi.org/10.1038/nsmb.1553.
[33] R. Durigon, Q. Wang, E. Ceh Pavia, C.M. Grant, H. Lu, Cytosolic thioredoxin system facilitates the import of mitochondrial small Tim proteins, EMBO Rep. 13 (2012) 916–922, https://doi.org/10.1038/embor.2012.116.
[34] K. Kojer, M. Bien, H. Gangel, B. Morgan, T.P. Dick, J. Riemer, Glutathione redox potential in the mitochondrial intermembrane space is linked to the cytosol and impacts the Mia40 redox state, EMBO J. 31 (2012) 3169–3182, https://doi.org/10.1038/emboj.2012.165.
[35] L.W. Thomas, J.M. Stephen, C. Esposito, S. Hoer, R. Antrobus, A. Ahmed, H. Al-Habib, M. Ashcroft, CHCHD4 confers metabolic vulnerabilities to tumour cells through its control of the mitochondrial respiratory chain, Canc. Metabol. 7 (2019) 1–18, https://doi.org/10.1186/s40170-019-0194-y.
[36] H. Fraga, S. Ventura, Oxidative folding in the mitochondrial intermembrane space in human health and disease, Int. J. Mol. Sci. 14 (2013) 2916–2927, https://doi.org/10.3390/ijms14022916.
[37] S.E. Neal, D.V. Dabir, J. Wijaya, C. Boon, C.M. Koehler, Osm1 facilitates the transfer of electrons from Erv1 to fumarate in the redox-regulated import pathway in the mitochondrial intermembrane space, Mol. Biol. Cell 3 (2017), https://doi.org/10.1091/mbc.E16-10-0712 mbc.E16-10-0712.
[38] R.S. Balaban, S. Nemoto, T. Finkel, Mitochondria, oxidants, and aging, Cell 120 (2005) 483–495, https://doi.org/10.1016/j.cell.2005.02.001.
[39] W. Dröge, Free radicals in the physiological control of cell function, Physiol. Rev. 82 (2002) 47–95, https://doi.org/10.1152/physrev.00018.2001.
[40] H.C. Ha, a Thiagalingam, B.D. Nelkin, R. a Casero, Reactive oxygen species are critical for the growth and differentiation of medullary thyroid carcinoma cells, Clin. Canc. Res.: An Official Journal of the American Association for Cancer Research 6 (2000) 3783–3787.
[41] J.W. Baynes, Role of oxidative stress in development of complications in diabetes, Diabetes 40 (1991) 405–412, https://doi.org/10.2337/diab.40.4.405.
[42] R. Kinscherf, M. Wagner, H. Kamencic, G.A. Bonaterra, D. Hou, R.A. Schiele, H. P. Deigner, J. Metz, Characterization of apoptotic macrophages in atheromatous tissue of humans and heritable hyperlipidemic rabbits, Atherosclerosis 144 (1999) 33–39, https://doi.org/10.1016/S0021-9150(99)00037-4.
[43] Y. Kushnareva, A.N. Murphy, A. Andreyev, Complex I-mediated reactive oxygen species generation: modulation by cytochrome c and NAD(P)+ oxidation-reduction state, Biochem. J. 368 (2002) 545–553, https://doi.org/10.1042/BJ20021121.
[44] Q. Chen, E.J. Vazquez, S. Moghaddas, C.L. Hoppel, E.J. Lesnefsky, Production of reactive oxygen species by mitochondria, J. Biol. Chem. 278 (2003) 36027–36031, https://doi.org/10.1074/jbc.M304854200.
[45] M.D. Shelton, J.J. Mieyal, Regulation by reversible S-glutathionylation: molecular targets implicated in inflammatory diseases, Mol. Cell. 25 (2008) 332–346, 74 [pii].
[46] D.P. Jones, H. Sies, The redox code, Antioxidants Redox Signal. 23 (2015) 734–746, https://doi.org/10.1089/ars.2015.6247.